

From the data presented in this paper, several conclusions can be drawn. 1) Electron densities in excess of  $10^{10}/\text{cm}^3$  are found several meters in front of shock waves travelling in air at velocities greater than 10 km/sec. 2) High reflectivity of the shock-tube wall significantly enhances the precursor electron density. 3) Driven gas impurities play a major role in the photo-ionization in pure nitrogen ahead of shock waves traveling at velocities greater than 10 km/sec. Air data, however, are much less sensitive to impurities. 4) For the shock velocity range investigated herein,  $10 < V < 13$  km/sec, the precursor electron densities at initial pressures of 0.2 and 0.4 torr appear to be proportional to the eighth power of shock velocity whereas at an initial pressure of 0.1 torr the data appear to be proportional to the seventh power of velocity.

### References

- <sup>1</sup> Holmes, L. B. and Weyman, H. D., "Plasma Density Ahead of Pressure Driven Shock Waves," *Proceedings of the Fifth International Shock Tube Symposium*, Silver Spring, Md., 1965, p. 93.
- <sup>2</sup> Lederman, S. and Wilson, D., "Microwave Resonance Cavity Measurements of Shock Produced Electron Precursors," *AIAA Journal*, Vol. 5, No. 1, Jan. 1967, pp. 70-77.
- <sup>3</sup> Glick, H. S., "Microwave Study of Electron Precursors," *Bulletin of the American Physical Society*, Vol. 13, No. 11, Nov. 1968, p. 1518.
- <sup>4</sup> Presley, L. L., Falkenthal, G. E., and Naff, J. T., "A 1 MJ Arc Discharge Shock Tube as a Chemical Kinetics Research Facility," *Proceedings of the Fifth Shock Tube Symposium*, Silver Spring, Md., 1965, p. 857.
- <sup>5</sup> Heald, M. A., and Wharton, C. B., *Plasma Diagnostics with Microwaves*, Wiley, New York, 1965, pp. 192-204.
- <sup>6</sup> Dobbins, R. A., "Photoexcitation and Photoionization of Argon ahead of a Strong Shock Wave," *AIAA Paper 68-666*, Los Angeles, Calif., 1968.

## Investigations of Flow in Triangular Cavities

T. P. TORDA\* AND B. R. PATEL†

*Illinois Institute of Technology, Chicago, Ill.*

### Introduction

THE experimental investigations presented are directed toward the study of flow inside triangular-shaped cavities of variable depths, induced by either steady or starting flows over the cavity mouth. Of particular interest are the time-dependent fluctuations occurring at the mouth of the cavity that may excite acoustic oscillations. Triangular shapes were chosen because they resemble baffle cavities used in liquid propellant rocket motors. These baffle cavities serve to decouple the injector from the rest of the combustion chamber where longitudinal, tangential, and radial modes of oscillations, or a combination of these, occur. The experimental setup simulated radial and tangential modes of oscillations over the cavities.

### Experimental Setup and Techniques

The triangular cavity to be investigated was attached to the lower face of the test section of a specially designed wind tunnel. The direction of the airflow over the cavity is shown in Fig. 1. Two Plexiglass cavities were used, and the depths

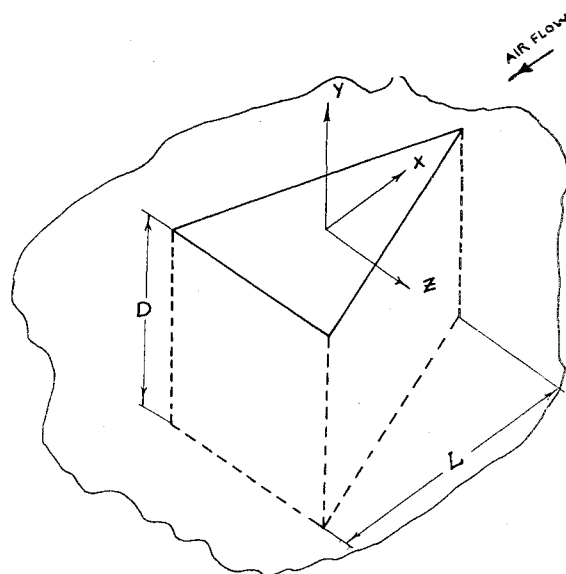


Fig. 1 Schematic diagram of the cavity.

of these cavities could be varied from 0 to 25 in. The apex angles of the triangular cavities were  $60^\circ$  and  $30^\circ$ , respectively, and each had a 10-in. base. The flow velocity was low subsonic ( $0.10 < M < 0.20$ ), and the Reynolds number based on the height of the wind-tunnel cross section was  $4.25 \times 10^4$  and larger. Hence, the flow regime was turbulent.

To understand the nature of the secondary flow induced in the cavity, it is necessary to know 1) whether the flow is steady or time-dependent, 2) the number and the size of the vortices formed in the cavity, 3) the position of these vortices, and so on. Various measurement techniques such as hot-wire anemometry, use of pressure probes for pressure measurements, flow visualization techniques, etc. may be used. Flow visualization is a fairly reliable tool in obtaining physical insight into flow regimes.

Flow visualization by injecting smoke into the air stream was tried but proved to be impractical because of rapid diffusion caused by the high level of turbulence existing at the mouth of the cavity. Hence, particles were used instead. The particles were the 3S grade of industrial "Perlites." Perlites are compounds of  $\text{SiO}_2$ ,  $\text{Al}_2\text{O}_3$ ,  $\text{K}_2\text{O}$ , and  $\text{NaO}$ . The bulk density of the 3S grade is 2.5 to 3 lbs/ft<sup>3</sup>, and 92% of the particles pass through No. 30 mesh.

For steady airstreams over the cavities, the particles were injected into the airflow upstream of the test section to obtain the cavity flow pattern. In order to study the starting vortices, a layer of particles was spread at the bottom of the cavity and the airflow then was started. The particles were photographed by both high-speed (2000 frames/sec) and standard-speed (18 frames/sec) movie cameras. A frame-by-frame analysis of the resulting film gave the flow patterns shown in Figs. 2-7. To provide a better insight into the three-dimensionality of the flow, the flow patterns were photographed in both from the X direction and from the Z direction (Fig. 1).

### Results and Discussion

Some of the flow patterns for the  $60^\circ$  apex-angle cavity as viewed from the Z direction are shown in Figs. 2-5 (the flow is from right to left). Figures 2-4 show the flow patterns in a typical shallow cavity ( $L/D > 2$ ). The pattern shown in Fig. 2 is predominant. However, small vortices are formed intermittently near the apex as shown in Figs. 3 and 4. These small vortices are swept from the cavity and are reformed aperiodically. Figure 6 shows the same cavity, viewed from the X direction. The flow pattern clearly shows the three-dimensionality of the flow. There are two main vortices

Received May 21, 1969; revision received August 13, 1969. This research was supported by Air Force Office of Scientific Research, Office of Aerospace Research, U.S. Air Force.

\* Professor, Department of Mechanical and Aerospace Engineering. Associate Fellow AIAA.

† Research Assistant, Department of Mechanical and Aerospace Engineering.

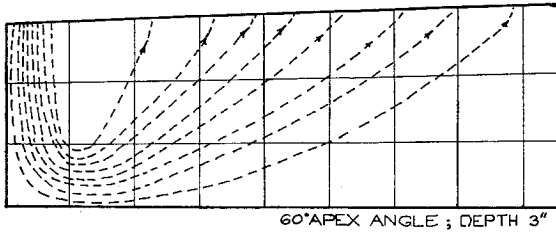


Fig. 2 Flow pattern in the 3-in.-deep 60° apex-angle cavity.

along the two sides of the cavity. The dotted lines show the region where unstable secondary vortices are formed. Figure 5 shows the flow typical of a deep cavity ( $L/D < 2$ ). There are one strong primary vortex and two secondary vortices. This pattern is quite stable in contrast to the unstable flow pattern in shallow cavities. Figure 7 shows the same cavity viewed from the  $X$  direction.

The flow patterns in deep and shallow 30° apex-angle cavities are similar to those in the 60° apex-angle cavity. The 60° apex-angle cavity was found to resonate at a certain depth. The shear layer at the mouth of the cavity was explored with a hot-wire anemometer to record the oscillations occurring in that region. A periodic disturbance was found to exist in the shear layer with a frequency the same as the resonant frequency of the 60° apex-angle cavity. For deep cavities ( $L/D < 2$ ), one frequency was found to be predominant, though weak higher-order harmonics were present. When the depth of the cavity is such that resonance occurs, the frequency of the disturbance in the shear layer is pure and nearly free of higher harmonics. However, for shallow cavities the frequency of the disturbance is a composite of many harmonics. For the 30° apex-angle cavity, the frequency of the disturbance at the mouth of the cavity is irregular. This suggests that the mouth geometry strongly affects the disturbance frequency.

The frequency of the oscillations can be predicted by the empirical expression attributed to Strouhal,

$$f = \alpha (V/L)n, \text{ where } n = 1, 2, 3, 4 \dots$$

Here,  $f$  = frequency in cycles/sec;  $V$  = velocity of the primary exciting flow, fps;  $L$  = characteristic length, ft, in this case the height of the triangular cross section; and  $\alpha$  = dimensionless number known as the Strouhal number, which is determined experimentally. The value of  $\alpha$  for the 60° apex-angle cavity was found to be 0.47 when the value of  $n$  was 4. Hence, for the 60° apex-angle cavity the frequency of the disturbances at the mouth of the cavity could be predicted by

$$f = 4 \alpha V/L \quad (1)$$

The experimentally determined value for the depth at which the 60° apex-angle cavity resonates agrees closely with the depth predicted by the theoretical analysis made for a closed end resonator by Blokhintsev<sup>1</sup> as follows.

The displacement  $\xi$  of the air along the  $Y$  axis is subject to the wave equation

$$(\partial^2 \xi / \partial t^2) + c^2 \delta (\partial \xi / \partial t) - c^2 (\partial^2 \xi / \partial x^2) = 0 \quad (2)$$

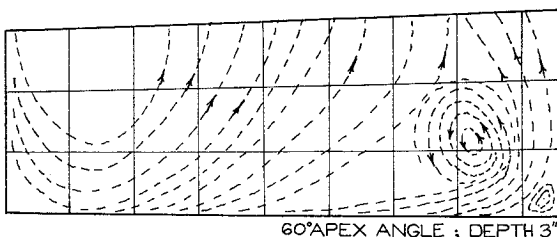


Fig. 3 Flow pattern in the 3-in.-deep 60° apex-angle cavity.

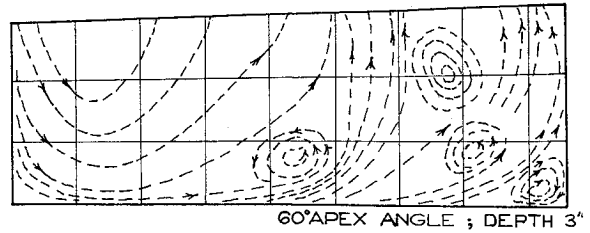


Fig. 4 Flow pattern in the 3-in.-deep 60° apex-angle cavity.

where  $\delta$  is the friction coefficient that takes into account the losses due to heat conduction and viscosity of the air, and  $c$  is the velocity of sound in air. The pressure at each point in the cavity is then given by

$$p(y, t) = -\rho c^2 (\partial \xi / \partial y) \quad (3)$$

Equation (2) must be solved for the boundary conditions

$$(\xi)_{y=0} = 0 \quad (4)$$

$$-\rho c^2 (\partial \xi / \partial y)_{y=D} = P(t) \quad (5)$$

The first boundary condition expresses the fact that at the closed end of the resonator ( $y = 0$ ) the air is at rest. The second condition indicates that at the mouth of the resonator the pressure is equal to the disturbance pressure  $P(t)$ , where  $P(t)$  is assumed to be sinusoidal with a frequency  $\omega$ . If the fact that the air at the mouth of the resonator takes part in the vibrations is taken into account, the last boundary condition can be modified to

$$-\rho c^2 (\partial \xi / \partial y)_{y=D} = \rho c (X + iY) (\xi)_{y=D} + P(t) \quad (6)$$

where  $X + iY$  is the impedance of the vibrating mass of air at the mouth of the resonator, generally termed as the mouth impedance, and  $\rho c (X + iY) (\xi)_{y=D} = P_1(t)$  is the pressure representing the reaction of the associated mass of air.

The active part of the impedance,  $X$  is due to the losses in radiation, while the reactive part  $Y$  is determined by the mass of the air vibrating along the resonator. The magnitudes of  $X$  and  $Y$  for a resonator with the area of the mouth  $s$  (these have been experimentally determined by Y. L. Gutin<sup>2</sup>) are equal to

$$X = (\omega^2 s / 4\pi c^2); \quad Y = 0.7(\omega/c) \cdot (s/\pi)$$

The solution yields the following condition for resonance

$$D = (1/k) \tan^{-1}(1/Y) \quad (7)$$

where  $k = \omega/c$ .

For the 60° apex angle cavity  $Y = 0.596$ , and at resonance  $k = 2.76$  rad/ft. Substituting these values of  $D$  and  $k$  in the above condition (7), we obtain  $D = 4.5$  in. The experimentally determined value of  $D$  is 5 in. Hence, the value

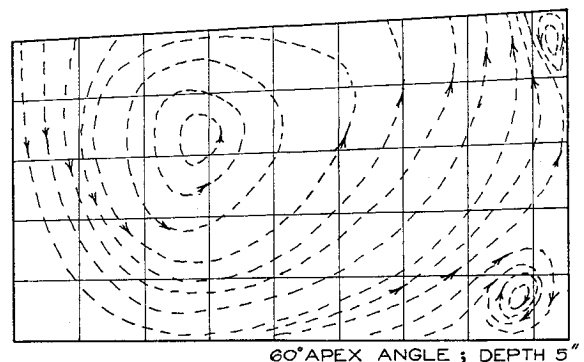
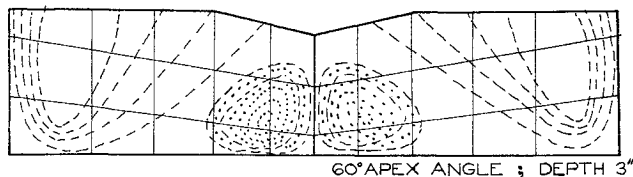


Fig. 5 Flow pattern in the 5-in.-deep 60° apex-angle cavity.



**Fig. 6 Flow pattern in the 3-in.-deep 60° apex-angle cavity viewed from the base of the triangular cross section.**

determined from Blokhintsev's analysis is in close agreement with the experimentally determined value.

### Conclusion

The conclusions drawn from this study are as follows.

1) When the depth of the cavity is shallow ( $L/D > 2$ ) the flow is very unstable, particularly near the apex of the cavity. In some instances as many as four secondary vortices were observed in the cavity. The formation of these vortices is not periodic; also, they are extremely unstable.

2) In deep cavities ( $L/D < 2$ ) the flow is quite stable. There is one main vortex present, and a couple of small secondary vortices at the apex of the cavity. As the cavity depth is increased, a second vortex appears beneath the main vortex.

3) Periodic oscillations are present in the shear layer at the mouth of the cavity. These oscillations may be due to periodic vortex shedding at the mouth of the cavity. For deep cavities there is one predominant frequency; however, for shallow cavities no single frequency is predominant and a whole spectrum of frequencies is present. The frequency of the oscillations depends on the mouth geometry and the exciting airstream velocity.

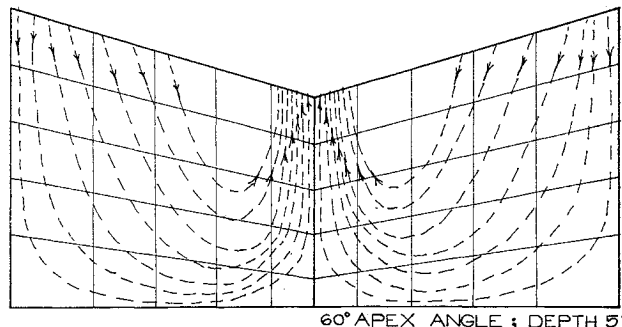


**Fig. 7 Flow pattern in the 5-in.-deep 60° apex-angle cavity viewed from the base of the triangular cross section.**

4) The frequency of oscillations for the 60° apex-angle cavity is given by the expression  $f = 4 \alpha (V/L)$  where  $\alpha = 0.47$ .

The depth of the cavity at which resonance occurs, predicted from Blokhintsev's<sup>1</sup> analysis, closely matches the value obtained experimentally. The 30° apex-angle cavity did not resonate at all. This indicates that the oscillations occurring at the mouth of the cavity are dependent on the mouth geometry.

### References

- <sup>1</sup> Blokhintsev, D. I., "Acoustics of a Homogeneous Moving Medium," TM 1399, Feb. 1956, NACA.
- <sup>2</sup> Gutin, Y. L., "Zvukovoe Pole Porshnebykh Izluchatelei," *Zhurnal Tekhnicheskoi Fiziki*, Vol. 7, 1937, p. 1096.